An in-vacuum x-ray diffraction microscope for use in the 0.7–2.9 keV range

D. J. Vine,[1,2,3,a)] G. J. Williams,[1,4] J. N. Clark,[1,5,6] C. T. Putkunz,[1,2] M. A. Pfeifer,[1,7] D. Legnini,[3] C. Roehrig,[3] E. Wrobel,[3] E. Huwald,[5] G. van Riessen,[1,5] B. Abbey,[1,2] T. Beetz,[8,b)] J. Irwin,[8] M. Feser,[8] B. Hornberger,[8] I. McNulty,[3] K. A. Nugent,[1,2] and A. G. Peele[1,5,c)]

[1]*Australian Research Council Centre of Excellence for Coherent X-ray Science, Australia*
[2]*School of Physics, The University of Melbourne, Victoria 3010, Australia*
[3]*Argonne National Laboratory, Argonne, Illinois 60439, USA*
[4]*SLAC National Accelerator Laboratory, Menlo Park, California 94025, USA*
[5]*Department of Physics, La Trobe University, Bundoora, Victoria 3086, Australia*
[6]*London Centre for Nanotechnology, University College, London WC1E 6BT, United Kingdom*
[7]*Cornell High Energy Synchrotron Source, Cornell University, Ithaca, New York 14850, USA*
[8]*Xradia, Inc., 4385 Hopyard Road, Pleasanton, California 94588, USA*

(Received 1 June 2011; accepted 6 February 2012; published online 14 March 2012)

A dedicated in-vacuum coherent x-ray diffraction microscope was installed at the 2-ID-B beamline of the Advanced Photon Source for use with 0.7–2.9 keV x-rays. The instrument can accommodate three common implementations of diffractive imaging; plane wave illumination; defocused-probe (Fresnel diffractive imaging) and scanning (ptychography) using either a pinhole, focused or defocused probe. The microscope design includes active feedback to limit motion of the optics with respect to the sample. Upper bounds on the relative optics-to-sample displacement have been measured to be 5.8 nm(v) and 4.4 nm(h) rms/h using capacitance micrometry and 27 nm/h using x-ray point projection imaging. The stability of the measurement platform and in-vacuum operation allows for long exposure times, high signal-to-noise and large dynamic range two-dimensional intensity measurements to be acquired. Finally, we illustrate the microscope's stability with a recent experimental result. © *2012 American Institute of Physics*. [http://dx.doi.org/10.1063/1.3688655]

INTRODUCTION

Coherent diffractive imaging (CDI) with x-rays is a technique for high-resolution imaging at the nanoscale.[1–3] CDI is a two step imaging process in which the far-field diffraction pattern of a coherently illuminated sample is recorded in the first step and computationally reconstructed in a second, post-measurement step.[4,5] Among the advantages of this approach over scanning probe and full-field transmission x-ray microscopy techniques are the inherent ability to retrieve the complex amplitude of the sample's exit surface wave, the efficient use of all forward scattered photons from the sample, and coupling the image resolution to the numerical aperture of the detector rather than an objective lens. CDI performed with standard pixel array detectors can easily access a numerical aperture of 1 nm which is well beyond the current limits of x-ray optics fabrication.

In this paper, we describe an x-ray coherent diffraction microscope designed to provide an ultra-stable platform to minimise sample motion and a windowless vacuum environment to minimise background scattering. This dedicated instrument specialises in both plane wave and focused probe diffractive imaging experiments, Figure 1. It has been installed at the 2-ID-B beamline of the Advanced Photon Source.[6] The insertion device at 2-ID-B is a 5.5 cm period undulator and the beamline is optimised to deliver x-rays in the 0.7–2.9 keV energy range with a coherent flux of 10^9–10^{12} photons/s/0.1% BW (coherence lengths: 160 μm(h) × 2 mm(v)) to the focusing optic. This large coherent flux is well suited for imaging of materials and soft-biological samples and encompasses numerous absorption edges in the intermediate energy range between soft and hard x-rays.

Two important practical considerations for diffractive imaging which affect the accuracy, contrast and resolution of a CDI reconstruction are the stability of the sample with respect to the illuminating radiation,[7] and air scattering and absorption of the photons between the sample and the detector. Sample stability is critically important in scanning diffractive imaging using a pinhole,[8] focused probe[9] or defocused probe[10] imaging experiments. Sources of instability such as thermal expansion of the stage stacks can cause unacceptably large displacement errors over the course of a measurement if not corrected, for example, 100 mm of aluminum expands 2 μm/°C. Intra-exposure sample movement results in a blurred diffraction pattern while inter-exposure sample movement does not allow repeated exposures to be added to increase the dynamic range of the measurement.

We require the random motion of the sample be much smaller than the detector point spread function.[7] This can be achieved though both passive and active control of the illuminating optic. For this microscope we have found that passive

a)Author to whom correspondence should be addressed. Electronic mail: dvine@aps.anl.gov.
b)Present address: Center for Probing the Nanoscale, Stanford University, Stanford, California 94305, USA.
c)Present address: Australian Synchrotron, Clayton, Victoria 3168, Australia.

 © 2012 American Institute of Physics

Downloaded 14 Nov 2012 to 171.67.216.21. Redistribution subject to AIP license or copyright; see http://rsi.aip.org/about/rights_and_permissions

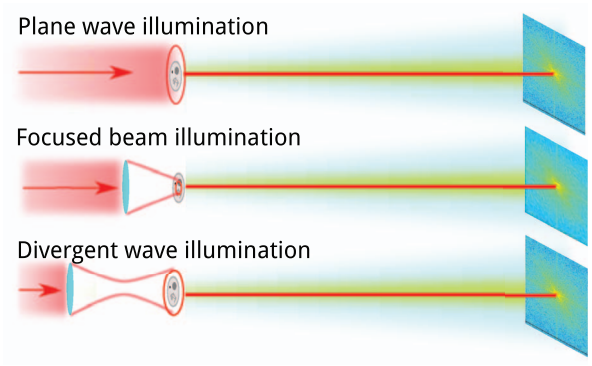

FIG. 1. (Color online) Overview of diffractive imaging techniques that can be implemented in the microscope. A plane wave illuminates an isolated sample and an area detector in the far field records the coherent diffraction pattern (top), the sample is placed in the focal plane of a zone plate lens (middle), the sample is illuminated with a divergent wave (bottom). All three methods can be used for single-view imaging whereas the bottom two techniques can be combined with ptychography to map out an extended field of view.

control alone is more effective and is sufficient to achieve the stability goal.

The *in vacuo* operation of the microscope minimises interaction of the scattered x-rays with air and vacuum windows. The instrument is directly coupled to the 2-ID-B beamline vacuum.

The energy range and resolution of this microscope make it well suited for studying fixed biological specimens such as single cells in three dimensions. To this end the sample stage is equipped with a high-resolution tomography rotation stage comprising a gold-coated metrology disk and five capacitive sensors for measuring the tip/tilt due to off-axis wobble so that it can be corrected computationally in a post-measurement step.

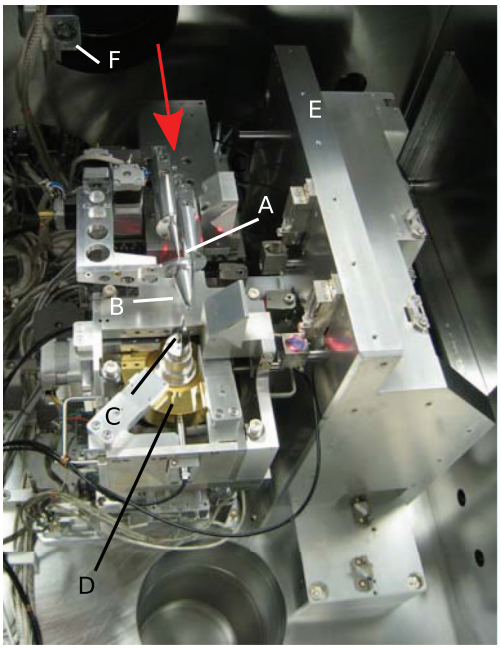

FIG. 3. (Color online) The interior of the vacuum chamber showing: A - the zone plate (obscured), B - the OSA, C - the sample, D - gold metrology disk, E - the aluminum reference, and F - the BDA stage.

MICROSCOPE DESIGN AND INSTRUMENTATION

A schematic diagram of the beamline and microscope and photos of the vacuum chamber are shown in Figures 2 and 3. The beamline and optics have been described in detail elsewhere.[6]

The microscope, a prototype built by Xradia, Inc. and La Trobe University, was designed to minimise vibration and drift using closed-loop interferometric control. Subsequent

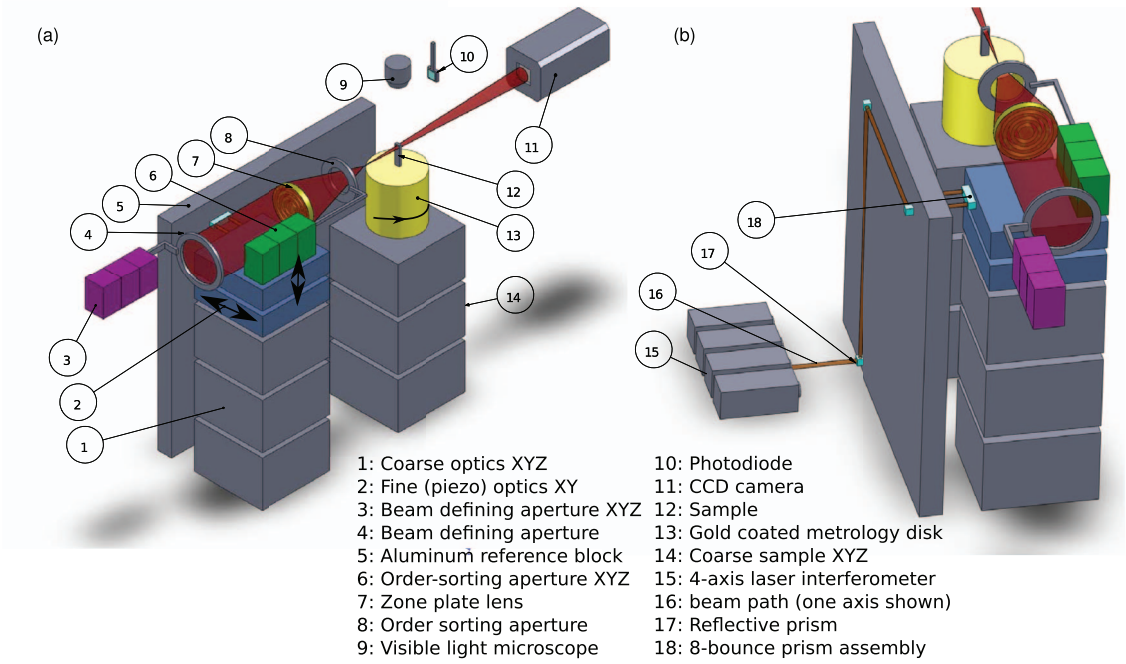

FIG. 2. (Color online) Schematic representation of the interior of the vacuum chamber. (a) Isometric view of the chamber. (b) Illustrating the optical interferometer. Only one axis of the interferometer is shown for clarity and the lasers (15) are external to the vacuum chamber.

Downloaded 14 Nov 2012 to 171.67.216.21. Redistribution subject to AIP license or copyright; see http://rsi.aip.org/about/rights_and_permissions

modification to the initial design and operation procedure have been implemented to optimize the performance and meet the demanding requirements of CDI.

The beam defining aperture (BDA) is a 1.5 mm diameter circular aperture used to reject parasitic scatter originating upstream in the beamline. X-rays passing through the BDA propagate to the focusing optics module (FOM) stack which holds the zone plate (ZP) and order sorting aperture (OSA). The ZP and OSA are mounted on left- and right-half cones, respectively, whose opening diameter is larger than the BDA. The BDA together with the ZP (and ZP-mounted central stop) and OSA pass only the first order focus from the ZP, thereby removing most of the parasitic scattering from sources upstream and minimising their impact on the reconstruction quality.

The beam which passes the FOM stack is incident on the sample (SAM) stack where it interacts with the sample before propagating to the detector. The detector is a Peltier cooled in-vacuum CCD (Princeton Instruments, PI-MTE) with 2048^2 13.5 μm pixels. Detection of infrared radiation from the stage position encoders and laser light from the interferometer is reduced by placing a 200 nm thickness aluminum on 200 nm parylene foil (Lebow Co.) a few centimetres upstream of the detector.

There are five groups of three-axis translation stages for the BDA, detector (DET), OSA, focusing optics (FOM) stack and sample (SAM) stack, respectively. These stages are used for coarse alignment and have approximately 1 μm resolution. The BDA, DET, and OSA stage stacks (Micos USA) are used in open-loop mode while the FOM and SAM (Newmark Systems, Inc., and Nanomotion Ltd.) use infrared encoders (Numerik Jena and Renishaw, respectively) for closed-loop control using a multi-axis motion controller (Delta Tau Data Systems, Inc.). All stages are actuated by stepper motors except for the x-, z-stages in the SAM and FOM stacks, which are piezo-walk servo-motor stages with 50 nm encoded resolution. The piezo-walk stages have the advantage of being compact, fast, and able to move heavy loads.

The BDA and DET z axes have longer travel (0.5 m and 0.8 m, respectively) than the other stages to give the greatest flexibility to use the microscope over the available energy spectrum. A rotary stage on the detector (National Apertures, Inc.) allows beamstops of different diameters to be inserted in front of the CCD to block the zero or first diffraction order from the zone plate.

Above the coarse translation stages in the SAM and FOM stacks are the rotation and weak-link piezo flexure stages,[11] respectively. The rotation stage is equipped with a gold plated metrology disc with five capacitive sensors to measure the wobble in the rotation for post-measurement processing and correction. The rotation is actuated with a stepper motor and achieves 1.4 μrad/step resolution. The weak-link flexure stage provides precision control (0.125 nm encoded, in practice 5 nm) of the optics with respect to the sample and is compatible with fast scanning.

Active control of the ZP optic with respect to the sample is made possible by measuring the x- and y-positions of the SAM and FOM stacks and positioning the weak-link stages to compensate for any relative change. A four-axis laser Doppler displacement measurement interferometer (Optodyne, Inc.[12]) records the displacement relative to a fixed reference point and the motion controller adjusts the weak-link piezo stage on the sample stack to achieve zero relative displacement. The optical path of a single (horizontal measurement) axis of the interferometer is shown in Figure 4.

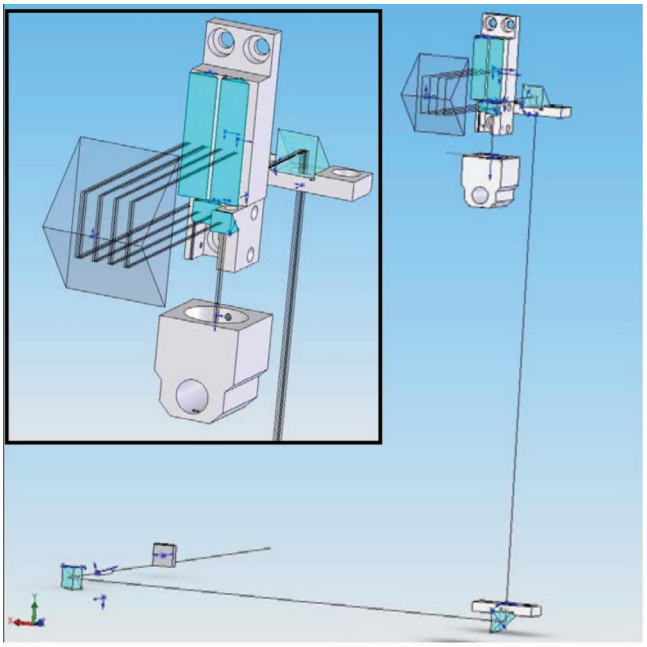

FIG. 4. (Color online) Schematic illustration of the optical path of one axis of the laser interferometer. The source and interferometer head are external to the vacuum chamber. The intermediate prisms are mounted on an aluminum reference block (not shown). The 8 reflections between the reference and measurement points result in an eight-fold increase in resolution.[21,22]

The visible light microscope (VLM) uses a caesium iodide scintillator and right-angle mirror in the sample position to reflect visible light to a long working distance objective CCD mounted on the roof of the chamber. The vacuum system consists of a roughing pump and turbopump which evacuate the chamber to 10^{-5} Torr within an hour.

Thermal stability was monitored using 10 channels of thermocouples placed in the interior and exterior of the vacuum chamber. The temperature was controlled passively by limiting access to the experimental hutch during measurements. The peak to peak fluctuation in the ambient temperature over a 24 h period was $\sim 1^{\circ}$.

INSTRUMENT PERFORMANCE

In practice we have found the interferometer system does not accurately measure the relative motion of the zone plate and sample. The cause of the instability is likely due to thermal expansion of the optics and their supports along the interferometer path.

The interferometer measures displacement relative to an aluminum reference frame which is assumed to provide a fixed reference point. However, due to thermal expansion the reference point moves a significant and measurable amount. Power consumption from four HeNe lasers external to the vacuum chamber (40 W) but thermally coupled to the

Downloaded 14 Nov 2012 to 171.67.216.21. Redistribution subject to AIP license or copyright; see http://rsi.aip.org/about/rights_and_permissions

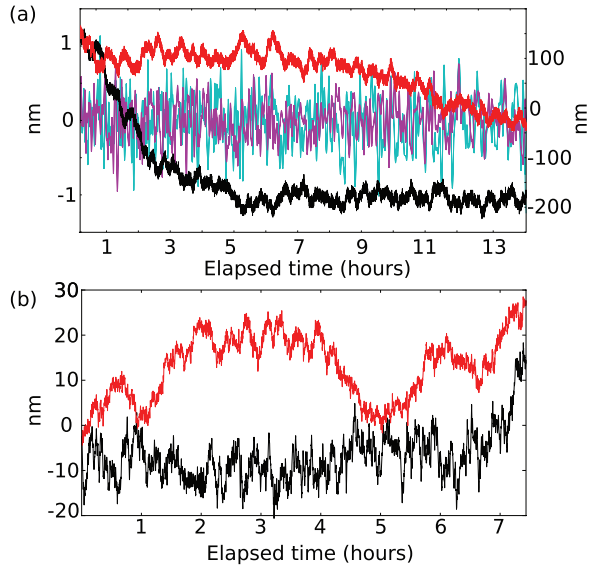

FIG. 5. (Color online) Stability of the microscope. (a) Illustrating thermal drifts of the interferometry reference point with closed loop. Left axis: relative ZP to sample displacement measured with interferometry, (middle overlapping traces). Right axis: The same measurement with capacitance micrometry, horizontal (bottom), vertical (top). (b) The relative displacement between zone plate and sample in passive mode measured with capacitive micrometry, horizontal (bottom), vertical (top).

chamber base and optical encoders integrated into the coarse motion stages (2 W) cause thermal gradients across the vacuum chamber. The thermal gradients are observed to not reach equilibrium over the course of several days. When the feedback loop is closed the interferometer then measures the thermal expansion of the reference block and actuates the piezo stage to compensate for the apparent relative ZP-sample motion, Fig. 5(a).

Capacitive displacement sensors were installed between the SAM and FOM stacks to give an independent verification of the interferometer displacement measurements. Two sensors were used to measure the horizontal and vertical displacements by attaching them rigidly to the SAM stack and using the surface of the FOM as the mating measurement point. The capacitive measurements were not used for closed loop feedback and were removed during experiments. The sensors were mounted to a short stainless steel arm (thermal expansion $\alpha = 0.5\,\mu$m/°K) far from heat sources. The actual measurement points were rigidly coupled to the points of interest (zone plate or sample) and there is assumed to be negligible motion between them.

We have been able to achieve excellent long term stability using only passive means as in Fig. 5(b), which shows the relative distance between ZP and sample as measured by capacitive micrometry. Figure 5(b) shows the RMS excursion from the mean position over a 7 h period is no greater than 4.4 nm (h) and 5.8 nm (v). We simultaneously measured point projection images with 500× magnification as an independent measurement of sample motion up to the resolution of the magnified pixels. There was no discernible motion over the seven hours from which we can infer the motion to be smaller than the image resolution of 27 nm which is in agreement with the capacitive micrometry.

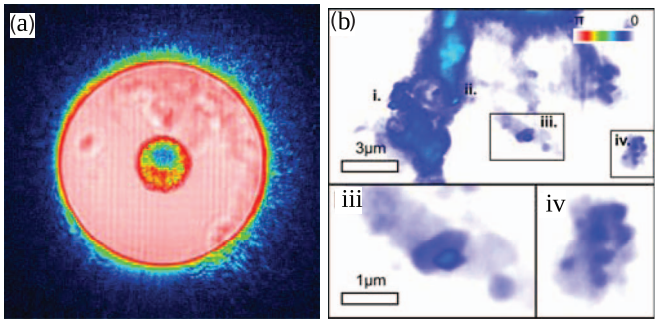

FIG. 6. (Color online) Imaging the sandcastle worm bio-adhesive. (a) A typical diffraction pattern and (b) high resolution reconstruction showing the internal structure of the adhesive. Reprinted from Ultramicroscopy, Vol. 111, C. T. Putkunz, J. N. Clark, D. J. Vine, G. J. Williams, E. Balaur, G. A. Cadenazzi, E. K. Curwood, C. A. Henderson, R. E. Scholten, R. J. Stewart, I. McNulty, K. A. Nugent, and A. G. Peele, Mapping granular structure in the biological adhesive of Phragmatopoma californica using phase diverse coherent diffractive imaging, 1184–1188, Copyright (2011), with permission from Elsevier.

RESULTS

We used the microscope successfully in a number of experiments[13–19] and this section highlights one experiment which illustrates the ultra-stability of the instrument.

The natural adhesive secreted by the sandcastle worm *Phragmatopoma californica* has the useful property of curing in sea water.[18,20] Reverse-engineering this adhesive could potentially lead to a way to set broken bones *in vivo*. A sample of the adhesive was studied by scanning it through the beam while recording a series of coherent diffraction patterns.[10] This type of experiment can only be conducted with an ultra-stable platform because it requires (i) repeated measurements due to the weak interaction of the biological sample with the incident x-rays and (ii) precise knowledge of the beam position on the sample for the reconstruction algorithm to succeed.

The sample was placed in 2.5 keV x-ray beam 1.72 mm beyond the focus of a 160 μm diameter zone plate optic with a 50 nm outermost zone width. The sample was raster scanned through a 25 position Cartesian grid with 84% overlap between adjacent positions covering a total area of 30 μm. The dataset was acquired over a period of 28 h and there was no discernible relative motion between the ZP and sample in any single position, which implies a drift smaller than 28 nm/h. Figure 6(a) shows the diffraction pattern from a single position in the scan with the bright central region being the hologram produced by interference between scattering from the sample and the first diffraction order of the zone plate. The ptychographic reconstruction is shown in Fig. 6(b) where we see the weakly interacting bio-adhesive is imaged in high resolution.

IMPROVEMENTS AND PLANNED UPGRADES

A key conclusion from the first two years operating this microscope is that even modest power dissipation close to critical components leads to instability and uncontrolled drift beyond the requirements of this instrument. With this in mind we have begun upgrading the microscope to minimise the

Downloaded 14 Nov 2012 to 171.67.216.21. Redistribution subject to AIP license or copyright; see http://rsi.aip.org/about/rights_and_permissions

reliance on active components (such as encoders) during data collection. The main changes are to replace the stages which must be operated in closed-loop (Nanomotion piezo-walk stages) with stepper driven stages, and replacing the interferometer system entirely. The new stepper driven stages will be operated open-loop with a half step resolution of 1 μm which can be combined with the weak link stage to achieve nanometre positioning accuracy without the use of optical encoders.

The interferometer will be redesigned with careful attention paid to ensuring that (i) the reference and measurement points are as close together as practicable, (ii) the interferometer is sensitive only to motion between the reference and measurement points, and (iii) the reference point is isolated thermally and mechanically from the stages and the rest of the chamber. When the reference point is not sufficiently isolated it cannot function as an independent measurement of sample drift and so cannot be used to correct it.

CONCLUSION

This paper describes the design and specifications of a dedicated in-vacuum diffraction microscope at beamline 2-ID-B at the Advanced Photon Source. The versatile design of the microscope allows for the sample to be illuminated using plane or divergent X-ray wavefields from ~50 nm to many micron in extent. We measured an upper bound to the relative stability of the zone plate with respect to the sample to be 27 nm/h by x-ray point-projection imaging and less than 6 nm/h by capacitance micrometry when the instrument was operated in passive mode, without interferometric stabilisation. The capacitance measurement provide an upper bound on the stability of the instrument, whereas the x-ray measurements directly quantify its capability for making high-resolution CDI measurements with high dynamic range. We anticipate further performance improvement with future upgrades to the x-ray diffraction microscope.

[1]J. Miao, D. Sayre, and H. N. Chapman, J. Opt. Soc. Am. A **15**, 1662 (1998).
[2]J. Miao, P. Charalambous, J. Kirz, and D. Sayre, Nature (London) **400**, 342 (1999).
[3]I. K. Robinson, I. A. Vartanyants, G. J. Williams, M. A. Pfeifer, and J. A. Pitney, Phys. Rev. Lett. **87**, 195505 (2001).
[4]K. A. Nugent, Adv. Phys. **59**, 1 (2010).
[5]H. M. Quiney, J. Mod. Opt. **57**, 1109 (2010).
[6]I. McNulty, A. Khounsary, J. Barraza, C. Benson, Y. P. Feng, and D. Shu, Rev. Sci. Instrum. **67**, 3372 (1996).
[7]G. J. Williams, H. M. Quiney, A. G. Peele, and K. A. Nugent, New J. Phys. **12**, 035020 (2010).
[8]H. M. L. Faulkner and J. M. Rodenburg, Ultramicroscopy **103**, 153 (2005).
[9]P. Thibault, M. Dierolf, A. Menzel, O. Bunk, C. David, and F. Pfeiffer, Science **321**, 379 (2008).
[10]D. J. Vine, G. J. Williams, B. Abbey, M. A. Pfeifer, J. N. Clark, M. D. De Jonge, I. McNulty, A. G. Peele, and K. A. Nugent, Phys. Rev. A **80**, 063823 (2009).
[11]D. Shu, T. S. Toellner, and E. E. Alp, Nucl. Instrum. Methods Phys. Res. A **467–468**, 771 (2001).
[12]C. Wang, Rev. Sci. Instrum. **71**, 3933 (2000).
[13]L. W. Whitehead, G. J. Williams, H. M. Quiney, D. J. Vine, R. A. Dilanian, S. Flewett, K. A. Nugent, A. G. Peele, E. Balaur, and I. McNulty, Phys. Rev. Lett. **103**, 243902 (2009).
[14]C. T. Putkunz, M. A. Pfeifer, A. G. Peele, G. J. Williams, H. M. Quiney, B. Abbey, K. A. Nugent, and I. McNulty, Opt. Express **18**, 11746 (2010).
[15]J. N. Clark, C. T. Putkunz, M. A. Pfeifer, A. G. Peele, G. J. Williams, B. Chen, K. A. Nugent, C. Hall, W. Fullagar, S. Kim, and I. McNulty, Opt. Express **18**, 1981 (2010).
[16]B. Abbey, L. W. Whitehead, H. M. Quiney, D. J. Vine, G. A. Cadenazzi, C. A. Henderson, K. A. Nugent, E. Balaur, C. T. Putkunz, A. G. Peele, G. J. Williams, and I. McNulty, Nat. Photonics **5**, 420 (2011).
[17]C. T. Putkunz, J. N. Clark, D. J. Vine, G. J. Williams, M. A. Pfeifer, E.
Balaur, I. McNulty, K. A. Nugent, and A. G. Peele, Phys. Rev. Lett. **106**, 013903 (2011).
[18]C. T. Putkunz, J. N. Clark, D. J. Vine, G. J. Williams, E. Balaur, G. A. Cadenazzi, E. K. Curwood, C. A. Henderson, R. E. Scholten, R. J. Stewart, I. McNulty, K. A. Nugent, and A. G. Peele, Ultramicroscopy **111**, 1184 (2011).
[19]J. N. Clark, C. T. Putkunz, E. K. Curwood, D. J. Vine, R. Scholten, I. McNulty, K. A. Nugent, and A. G. Peele, Opt. Lett. **36**, 1954 (2011).
[20]R. J. Stewart, J. C. Weaver, D. E. Morse, and J. H. Waite, J. Exp. Biol. **207**, 4727 (2004).
[21]D. Shu, U.S. Patent 6,822,733 (23 November 2004).
[22]D. Shu, J. Maser, B. Lai, S. Vogt, Y. Wang, C. Preissner, Y. Han, B. Tieman, R. Winarski, A. Smolyanitskiy, and G. B. Stephenson, Proc. SPIE **5877**, E1 (2005).

Downloaded 14 Nov 2012 to 171.67.216.21. Redistribution subject to AIP license or copyright; see http://rsi.aip.org/about/rights_and_permissions